

Article

Cellular Automaton Model for Pedestrian Evacuation Considering Impacts of Fire Products

Yuechan Liu, Junyan Li and Chao Sun *

School of Measurement and Communication Engineering, Harbin University of Science and Technology, Harbin 150080, China; liuyuechan@hrbust.edu.cn (Y.L.); 1605020211@stu.hrbust.edu.cn (J.L.)

* Correspondence: sunchao@hrbust.edu.cn

Abstract: To accurately simulate realistic pedestrian evacuation from a fire, a cellular automaton model of the dynamic changes in pedestrian movement parameters is developed in conjunction with fire dynamics software. The fire dynamics software is used to simulate the spread of smoke within the scene to obtain visibility and CO concentration data within the scene. We imported the smoke data into the cellular automata and adjusted the pedestrian movement speed over time, resulting in simulation data that closely align with reality. The results show that for the single-room scenario, as pedestrian density increased from 0.1 to 0.5 persons per square meter (p/m^2), the influence of the percentage of pedestrians familiar with their location on evacuation efficiency decreased from 44.93% to 24.52%. Conversely, in the multi-room scenario, it increased from 23.68% to 38.79%. The proportion of pedestrians less affected by smoke decreases and stabilizes as the CO yield increases. In the single-room scenario, when the CO yield is below 10%, the crowd with a low percentage of pedestrians familiar with the site is more affected by smoke than those with a high percentage. In the multi-room scenario, the victimization rate of the crowd follows an increasing-then-decreasing curve, ultimately stabilizing with changes in CO yield.

Keywords: cellular automata; safety evacuation; public safety; compartment fire



Citation: Liu, Y.; Li, J.; Sun, C. Cellular Automaton Model for Pedestrian Evacuation Considering Impacts of Fire Products. *Fire* **2023**, *6*, 320. <https://doi.org/10.3390/fire6080320>

Academic Editors: Lizhong Yang, Zhijian Fu and Yanqiu Chen

Received: 19 July 2023

Revised: 14 August 2023

Accepted: 14 August 2023

Published: 17 August 2023



Copyright: © 2023 by the authors. Licensee MDPI, Basel, Switzerland. This article is an open access article distributed under the terms and conditions of the Creative Commons Attribution (CC BY) license (<https://creativecommons.org/licenses/by/4.0/>).

1. Introduction

Pedestrian evacuation in large public buildings during fire incidents is complex and variable. Fires can result in severe injuries and property damage [1–3]. On the one hand, evacuating people from architectures with complex geometries poses challenges due to their unique characteristics. On the other hand, smoke rapidly spreads in large public buildings, potentially leading to a large number of casualties. Therefore, it is essential to establish an evacuation model that considers the evolving state of pedestrians at each moment, providing practical guidance for post-fire pedestrian evacuation.

To address the risks associated with conducting pedestrian evacuation experiments in fire scenarios, researchers often employ simulation methods. The PyroSim 2018 software that was developed based on FDS is widely used in academia to simulate fire spread, and the Pathfinder software is used to analyze pedestrian evacuation [4–10]. For instance, Longhui Liao et al. utilized PyroSim and Pathfinder to simulate underground evacuation and smoke flow in the Guangzhou International Financial City [11]. Similarly, Muchen Zhou et al. proposed a rational design strategy to mitigate fire evacuation issues in high-rise school buildings by integrating machine learning algorithms with simulation software [12]. Zhang Nian et al. combined BIM technology with subway station fire evacuations to optimize subway station layouts [13]. In comparison to Pathfinder, the cellular automaton (CA) model excels in simulating pedestrian state changes throughout the evacuation process. The CA model is a modeling approach first introduced by Von Neumann [14] et al. in 1966 to study discrete problems in time, state, and space. Wen GuoWeng et al. developed a CA-based model for emergency evacuations to predict evacuation phenomena in specific

emergency scenarios [15]. In the context of fire evacuation, Wang Chen et al. employed CA to establish an evacuation model for elderly individuals and proposed an optimization strategy for evacuating nursing homes during fires [16]. Fu Zhijian et al. employed the CA model to analyze the impacts of individual tendencies on crowd evacuation efficiency, considering uneven exit attractiveness [17]. Kontou Panagiota et al. applied CA modeling to an evacuation problem involving individuals with disabilities [18]. Miyagawa Daiki and Ichinose Genki discovered an optimal turnover rate for crowd evacuation by simulating cellular automata-based models [19]. Additionally, Mitsopoulou Martha et al. developed a pedestrian evacuation model capable of simulating pedestrian characteristics using a cellular automata approach [20].

However, most CA models established thus far primarily focus on analyzing changes in pedestrian states and casualties, without considering the real-time effects of smoke on pedestrians during the smoke-spreading process. Therefore, this paper employs FDS-based Pyrosim software to acquire fire product data, combines it with CA modeling to establish a pedestrian evacuation model, and simulates pedestrian evacuation behavior during the smoke-spreading process. By considering factors such as pedestrians' visual range, familiarity with the surroundings, and physical condition this study investigates pedestrian evacuation during the fire-spreading process to offer guidance for effective pedestrian evacuation management.

2. Model of Pedestrian Evacuation Considering the Effects of Fire Products

2.1. Introduction of Pyrosim

Fire dynamics simulation (FDS) is a powerful computational fluid dynamics tool developed by the National Institute of Standards and Technology based on the principles of large eddy simulation. Pyrosim, derived from FDS, is a visual simulation framework that converts the programming information of FDS into a graphical representation. This conversion allows researchers to perform fire-related computational studies more intuitively and easily. Pyrosim is able to accurately simulate smoke propagation and dynamic temperature changes in fire scenarios. In addition, it can record parameters, such as hazardous gas concentrations and visibility ranges in the scenario, throughout the FDS simulation process [21,22].

2.2. Impact of Fire Products on Pedestrian Evacuation

In emergency situations, pedestrians heavily rely on their sense of sight as the primary means of acquiring information. When pedestrians are unfamiliar with their surroundings, they depend primarily on safety evacuation signs to navigate and exit the area safely. However, the presence of obstructions hampers pedestrian visibility, and the smoke generated by a fire further reduces light transmission, making it difficult for pedestrians to observe and comprehend fire signs [23]. To simulate smoke propagation, Pyrosim is used to provide visibility values for each location in the scene. The values are imported into the cellular automaton and the visibility range of the pedestrians is determined by judging the pedestrians using Equations (1) and (2). Figure 1 shows a schematic diagram of the pedestrian visibility range. The cross symbolizes the pedestrian's position, the black area represents obstructing objects, and the gray area represents the extent of the pedestrian's visibility range.

$$a_i = k \cdot \left(l_i - \sqrt{(x_i - x)^2 + (y_i - y)^2} \right) \cdot \left(l_j - \sqrt{(x_i - x_j)^2 + (y_i - y_j)^2} \right) \quad (1)$$

$$M \in a_i \quad a_i > 0 \quad (2)$$

where: a_i is the visibility range of pedestrians to the target point in m ; k is the obstacle weight, and when there is an obstacle between the target point and pedestrians $k = 0$, otherwise $k = 1$; l_i is the visibility of the target point in m ; l_j is the visibility range of the lowest point of visibility on a straight line distance between the target point and pedestrians

in m ; (x_i, y_i) are the coordinates of the target point; (x_j, y_j) are the coordinates of the lowest point of visibility on a straight line distance between the target point and the pedestrians; (x, y) are the coordinates of the position of the pedestrians; and M is the collection of visible points for the pedestrians.

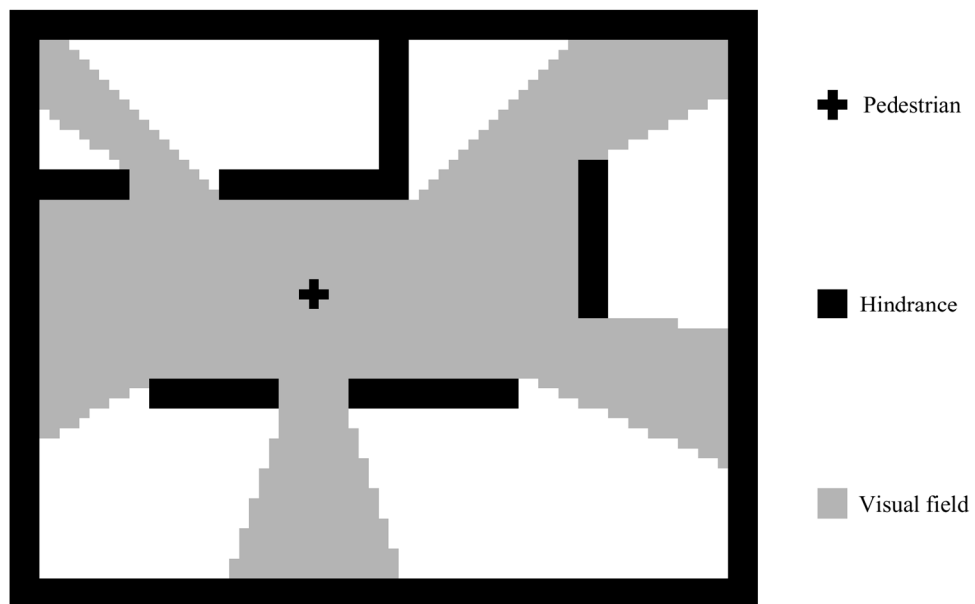


Figure 1. Visible area for pedestrians.

The influence of herd mentality is of great importance when studying pedestrian behavior in emergency evacuation scenarios [24]. Pedestrians tend to be influenced by the collective behavior of the crowd, causing them to move in the direction of the crowd's movement or gather with the crowd. Clustering by the fast search and find of density peaks (DPC), first proposed by Alex R and Alessandro L in 2014, is a method to quickly find data with the highest point density as clustering centroids [25]. In the context of pedestrian evacuation, the locations of pedestrians within the visual field are used as the dataset. By applying the DPC algorithm, pedestrians within the visual field are grouped into clusters, leveraging the herd mentality to direct their movement to clusters with the highest density. The center point of each cluster is calculated using Equations (3)–(5).

$$\rho_i = \sum_{i \neq j} \exp\left(-\frac{d_{ij}^2}{d_c^2}\right) \quad (3)$$

$$\delta_i = \begin{cases} \max(d_{ij}) & \rho_i = \max(\rho) \\ \min(d_{ij}) & \rho_i < \rho_j \end{cases} \quad (4)$$

$$\gamma_i = \rho_i \cdot \delta_i \quad (5)$$

where: d_{ij} is the distance between pedestrians at point i and other pedestrians j and m ; d_c is the truncation distance in m ; ρ_i is the pedestrian density at point i in p/m^2 ; ρ_j is the pedestrian density at point j in p/m^2 ; δ_i is the center offset distance in m ; and γ_i is the estimated value.

Fire produces a variety of pollutants that can pose a significant risk to human health. Analyzing the extent of damage to pedestrians after a fire incident involves assessing the concentration of these pollutants in their bodies. Carbon monoxide (CO) is one of the most common hazardous byproducts of fire [26]. However, the rate of CO production during combustion varies depending on the materials involved in the fire [27]. To shed light on the toxicology of CO, Qiu Rong and Fan Weicheng conducted an analysis that

established a relationship between the concentration of carboxyhemoglobin (HbCO) in the blood and the levels of CO in the surrounding air, as well as the duration of exposure, as shown in Table 1 [28]. To further investigate the impacts on pedestrians, this research employed the interpolation method to establish a correspondence between the rate at which the HbCO concentration increases in individuals and the concentration of CO in the surrounding environment.

Table 1. Relationship between CO concentration and inhalation time to blood HbCO concentration.

CO Concentration (mg/m ³)	Inhalation Period	HbCO Concentration (%)
230~340	5~6 h	23~30
460~690	4~5 h	36~44
800~1150	3~4 h	47~53
1260~1720	1.5~3 h	55~60
1840~2300	1~1.5 h	61~64
2300~3400	30~45 min	64~68
3400~5700	20~30 min	68~73
5700~11,500	2~5 min	73~76

The smoke produced by the fire combustion will affect the movement speed of the pedestrian [29], so to accurately simulate the movement process of the pedestrian, this paper adopts the dynamic time-step formula, which converts the speed of the pedestrian into the time that the pedestrian stays in the cell, and the time-step formula is shown in Equation (6):

$$ST = \frac{S}{v} \quad (6)$$

where: ST is the time of the pedestrian's stay; S is the size of the cell in m ; and v is the pedestrian's velocity in m/s .

Ye Chenghao et al.'s study summarized the effect of visibility and CO on the pedestrian's moving speed as shown in Equations (7) and (8) [30]:

$$f_s = \min(1, \max(0.2, 1 - 0.34 \cdot (3 - VIS))) \quad (7)$$

where: f_s is the visibility influence coefficient; and VIS is the visibility, m .

$$f_{CO} = \begin{cases} 1, & \rho < 0.1 \\ 1 - (0.2125 + 1.788\rho)\rho t, & 0.1 \leq \rho < 0.25 \\ 0, & \rho \geq 0.25 \end{cases} \quad (8)$$

where: f_{CO} is the coefficient of influence of CO in the fire products on the movement of pedestrians; ρ is the CO volume fraction in %; and t is the exposure time in min.

To calculate the effect of smoke on pedestrian velocity in a fire, Equation (6) is modified using Equations (7) and (8), and the modified relationship equation for the velocity variable is shown in Equation (9):

$$ST = \frac{S}{v \cdot f_s \cdot f_{CO}} \quad (9)$$

where: ST is the time of the pedestrian's stay; S is the size of the cell in m ; v is the speed of the pedestrian in m/s ; f_{CO} is the influence coefficient of CO on the pedestrian's movement; and f_s is the visibility influence coefficient.

2.3. Combining Cellular Automata Pedestrian Evacuation Modeling with Fire Dynamics Software

The CA model simplifies the site scenario into $N \times N$ cells and assigns different meanings to each cell. Pedestrians can move in the cells in different ways according to their state and environment. In this paper, the Moore-type neighborhood is chosen as the neighborhood of tuples in which pedestrians can move, and pedestrians in the Moore-type

neighborhood can choose one of the eight tuples around their tuple as a moving target, as shown in Figure 2.

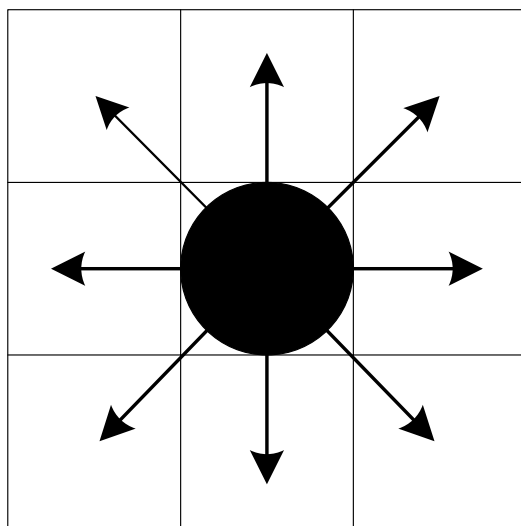


Figure 2. Moore neighborhood.

The size of each cell in the pedestrian evacuation model is set to $0.4\text{ m} \times 0.4\text{m}$. The room size of the single-room scenario is $13.2\text{ m} \times 10.4\text{ m}$. The multi-room model is a one-story rectangular place with a length of 38 m, a width of 18.4 m, and a floor height of 4 m. The place contains three adjacent rooms with dimensions of $13.2\text{ m} \times 10.4\text{ m}$, and each room has four exits with a width of 0.8 m connected to the corridor; the corridor has a width of 1.6 m and each side has one exit with a width of 2.4 m connected to the outside world. The scene model is shown in Figure 3. The PyroSim simulation software is used to create the fire model; the power of the fire source is set to 4 MW, visibility monitoring sensors and CO monitoring sensors are placed at a height of 1.8 m in the center of each cell, and the arrangement of the sensors is shown in Figure 4.

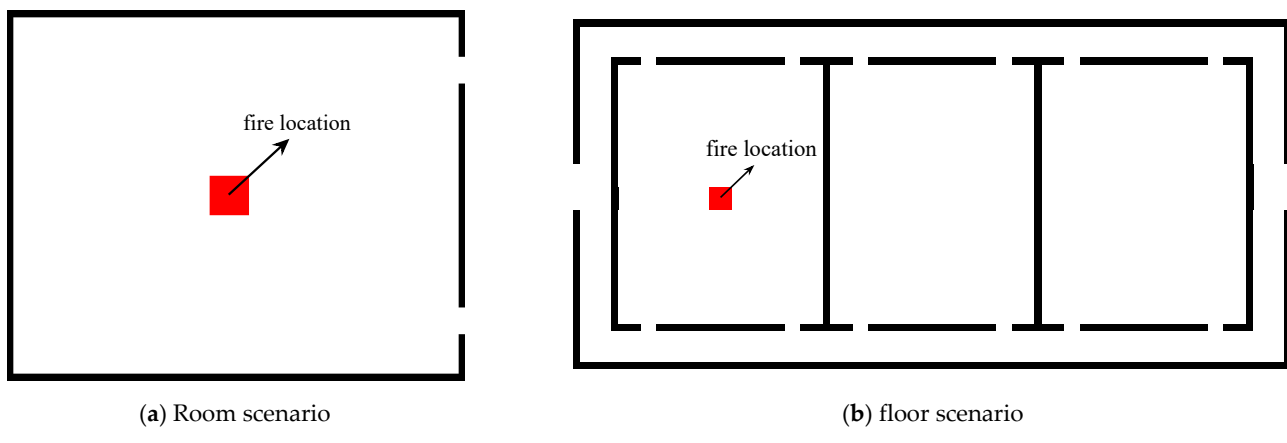


Figure 3. Simulation scenario.

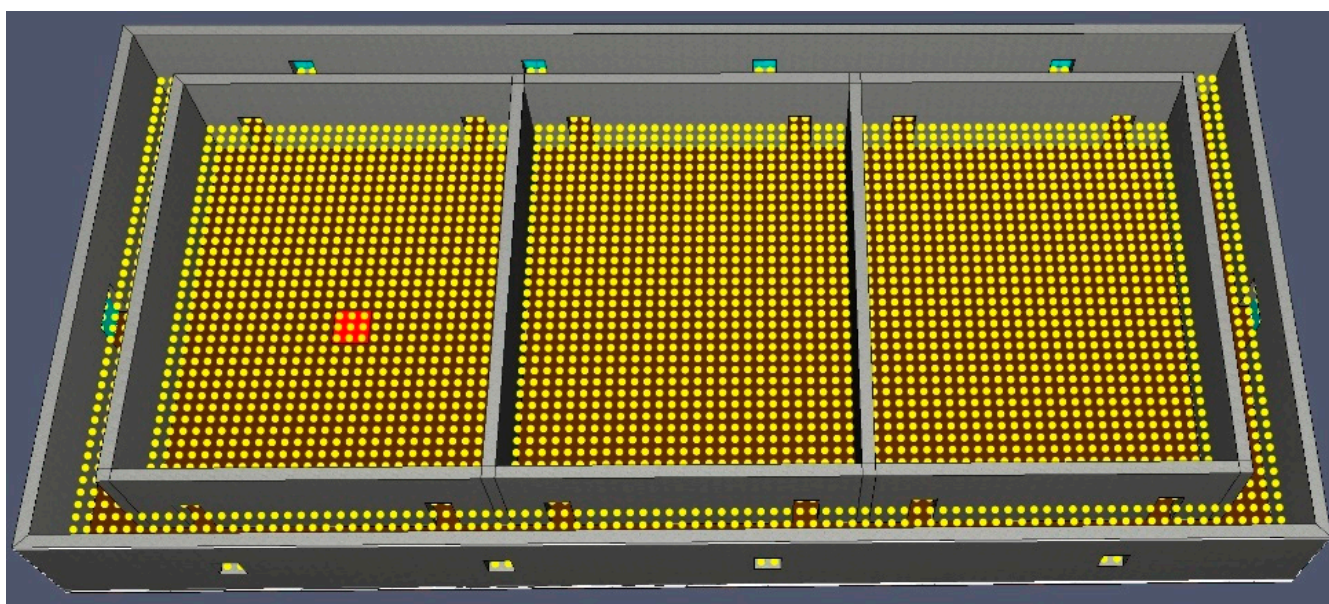


Figure 4. Sensor distribution within floor scenario.

Based on the traditional cellular automata model, this model is combined with Pyrosim software to obtain the smoke diffusion process in a fire, which more accurately simulates the environmental state of pedestrians at any moment. The iterative process of pedestrian movement in the CA-Pyrosim modeling algorithm is shown in Figure 5. The pedestrians to be evacuated are randomly distributed in the field. The undisturbed movement speed of the pedestrians is set to 1.2 m/s, and the pedestrians decide the movement mode according to the environment at each moment. The pedestrians in the scene were randomly divided into two categories: pedestrians familiar with the scene and pedestrians unfamiliar with the scene. In addition, the initial mental states of the pedestrians in the scene were randomly assigned so that the pedestrians were divided into two categories: pedestrians with rational mental responses and pedestrians with a herd mentality.

Figures 6–9 show the movement paths of pedestrians in different situations. Figure 6 shows the movement paths of pedestrians with different degrees of familiarity with the scene; pedestrians familiar with the scene will choose the shortest route to leave the scene, while pedestrians unfamiliar with the scene will choose to leave the scene along the wall when there is no reference. Figure 7 shows the movement paths of pedestrians following others in the herd mentality, where pedestrians will choose to follow the movement of others. Figure 8 shows the movement paths of pedestrians with herd mentality in the direction of crowd gathering, in which pedestrians with herd mentality do not follow the nearest pedestrians but choose to move toward the crowded place in the field of view. Figure 9 shows the movement paths of pedestrians after accounting for the smoke spread. As the smoke spreads, the pedestrians with the herd mentality and unfamiliar with the venue have a limited field of view due to smoke interference, and they cannot recognize the travelers in their field of view, so they move toward the wall and then leave the venue along the wall.

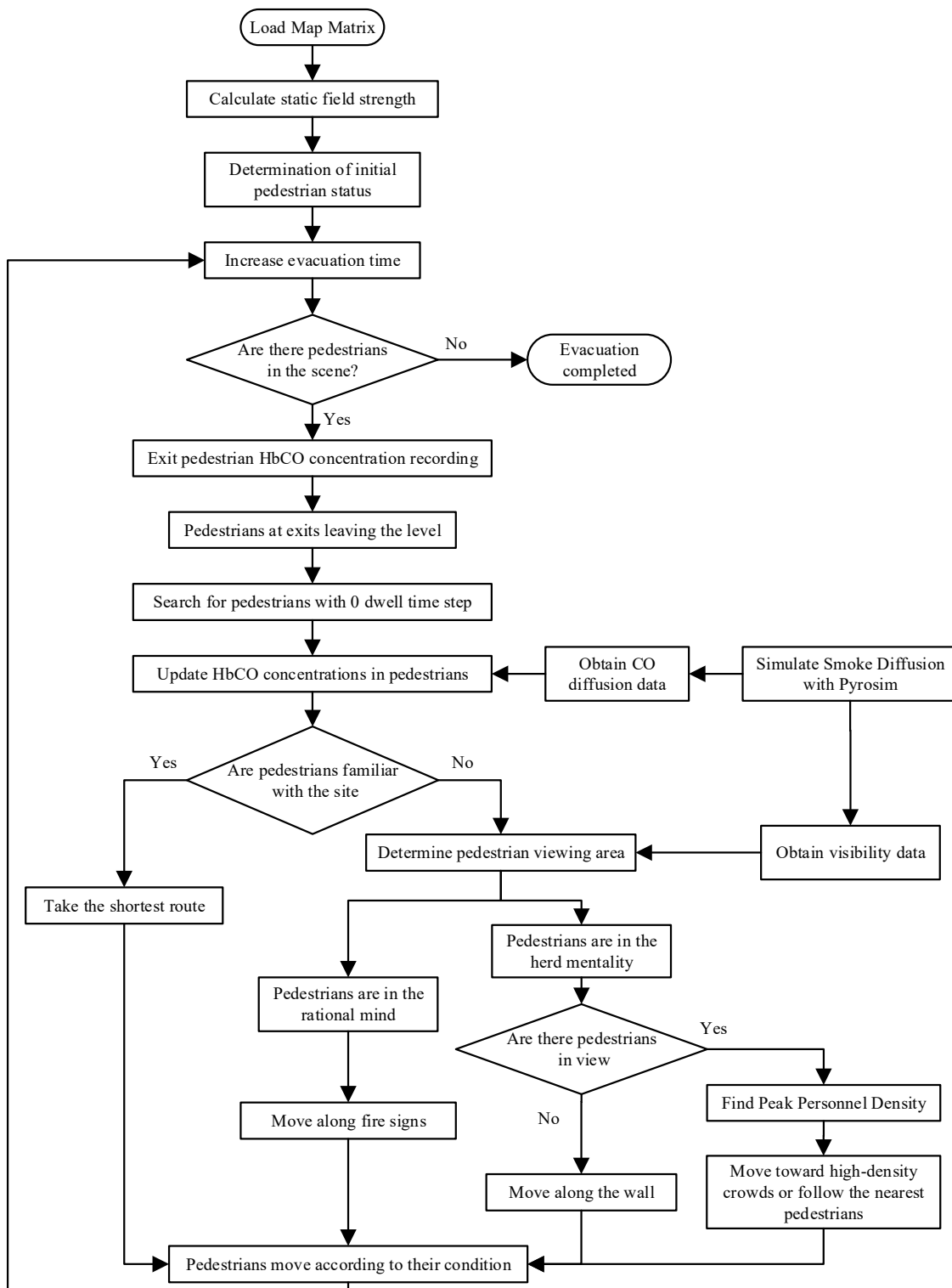


Figure 5. Flowchart of cellular automata.

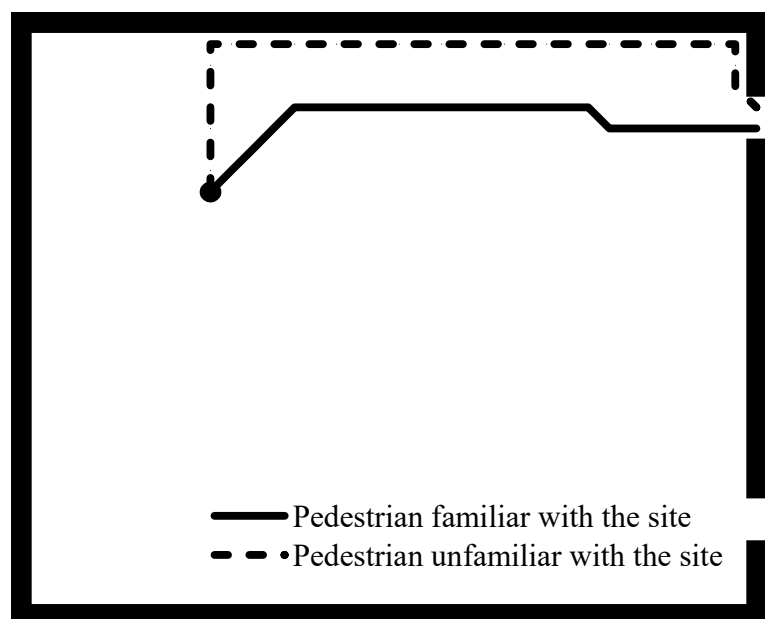


Figure 6. Movement paths of pedestrians familiar with the site.

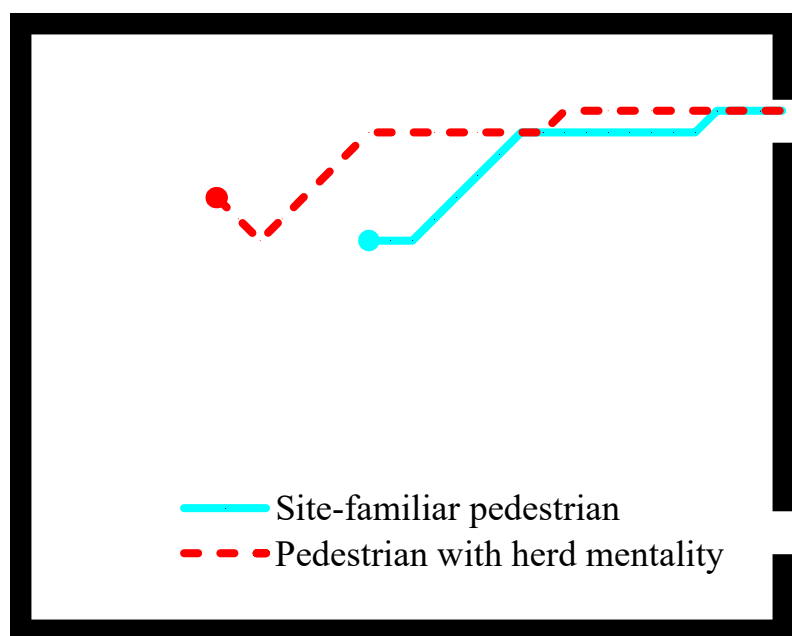


Figure 7. People with a herd mentality move with others.

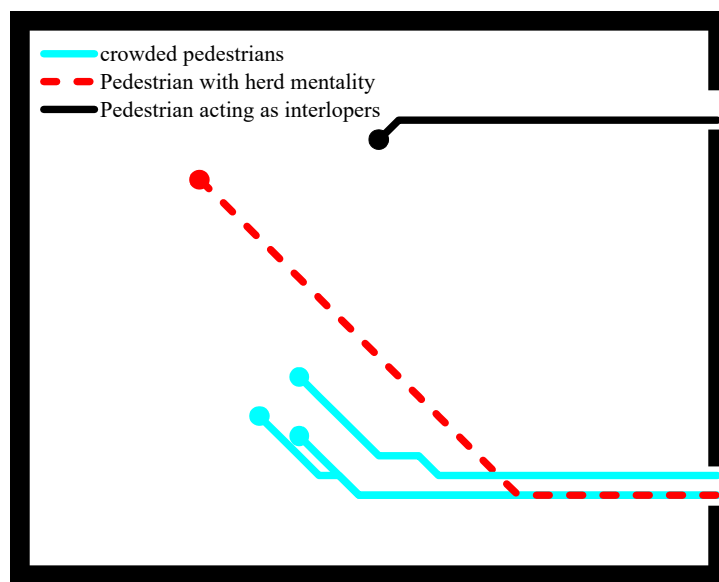


Figure 8. Pedestrian moves toward the gathering place.

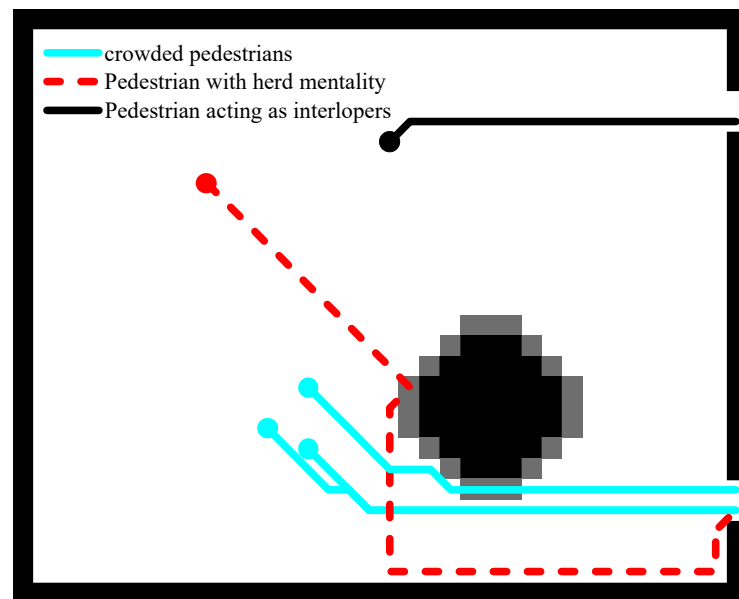


Figure 9. Movement paths of pedestrians when smoke spread.

3. Simulation and Results Analysis

3.1. Subsection Simulation Results

Figures 10 and 11 show the pedestrian evacuation schematic, where white cells represent pedestrians, gray cells represent open spaces, and black cells represent walls. Figure 10 shows the evacuation of 100 pedestrians in the indoor scenario. Because pedestrians can observe the exit locations and because the top and bottom exits in the room are equally attractive to pedestrians, pedestrians can exit the venue in an orderly fashion. Figure 11 shows the evacuation of 411 pedestrians in the multi-room scenario. As can be seen from Figure 10, the pedestrians walking along the walls in the corridor interfere with the evacuation of the pedestrians in the room, and at 27 s, the pedestrians in the middle room have finished evacuating, but the evacuation of the pedestrians on the two rooms on either side has not yet been completed. Due to the effects of herd mentality, the gathering phenomenon

of pedestrians will appear; the number of pedestrians gathered on the two sides of the room on both side doors is different.

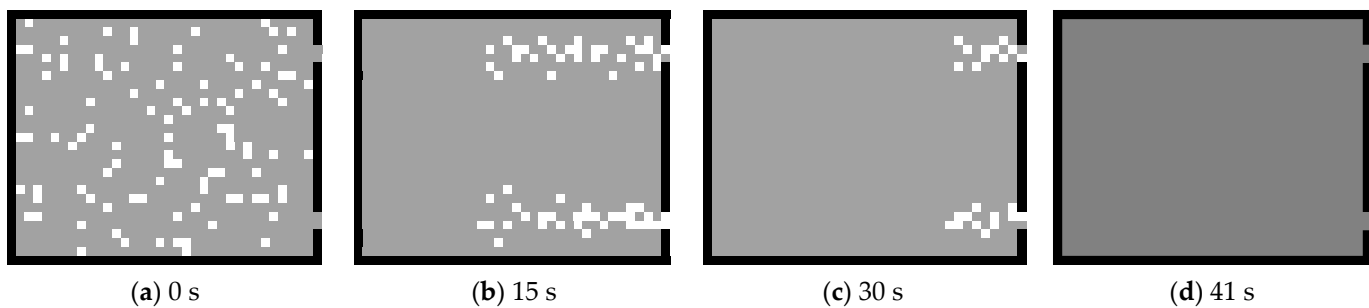


Figure 10. Pedestrian evacuation in room scenario.

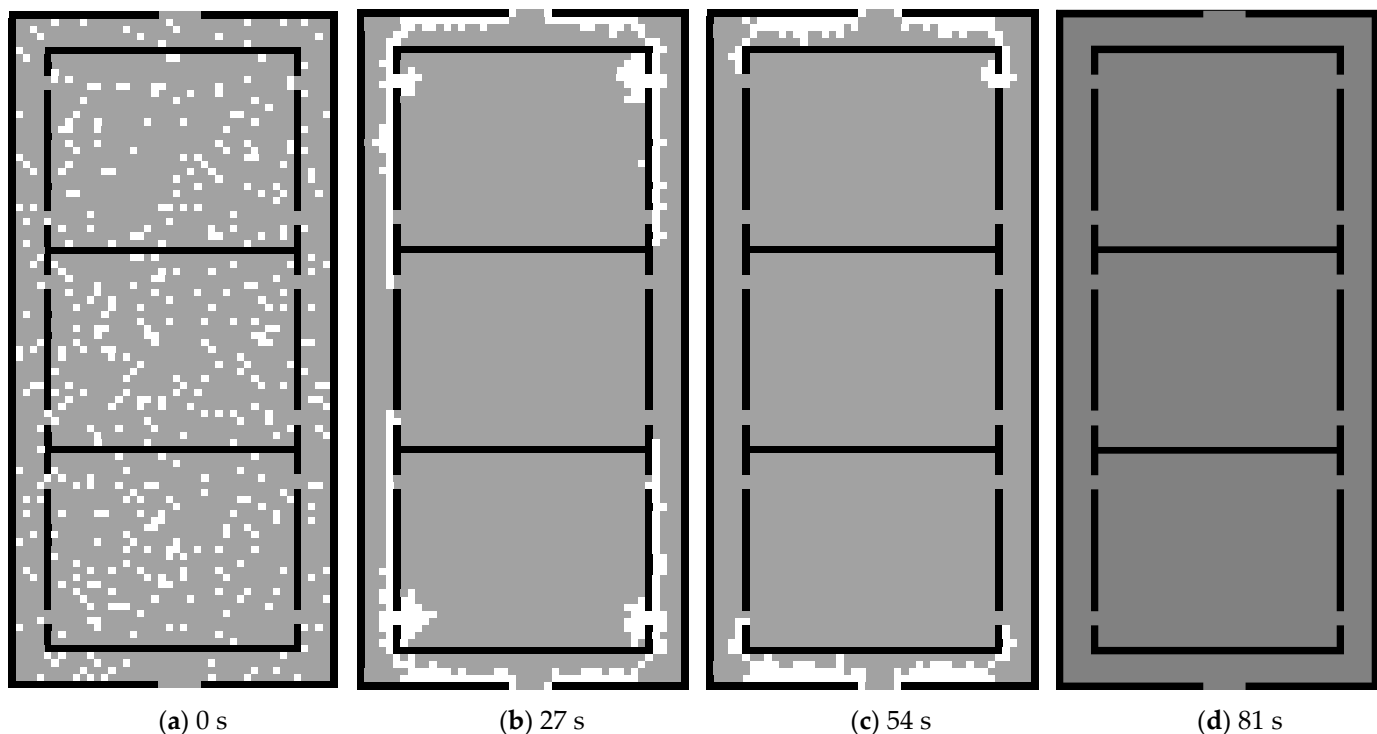


Figure 11. Pedestrian evacuation in floor scenario.

Smoke propagation in the multi-room scenario is shown in Figures 12 and 13. Figure 12 shows the visibility graph. At 15 s, the visibility at 1.8m in the room where the fire source is located decreases to zero, which severely affects the visibility of pedestrians. At 40 s, the visibility in the corridor next to the fire source room decreases to zero, and smoke begins to appear in the room without the fire source. At 80 s, the corridors were filled with smoke, and the smoke began to spread to the non-fire rooms. Figure 13 shows the schematic diagram of CO concentration distributions in a multi-room scenario. At 20 s, the CO concentration reached 0.25% in some areas of the fire source room, and the pedestrian velocity began to decrease. At 50 s, the volume fraction of CO in the fire room reached 0.5% and the moving speed of pedestrians is reduced to zero. At 80 s, the CO concentration in most corridors reached 0.25%, which adversely affected the overall evacuation effect.

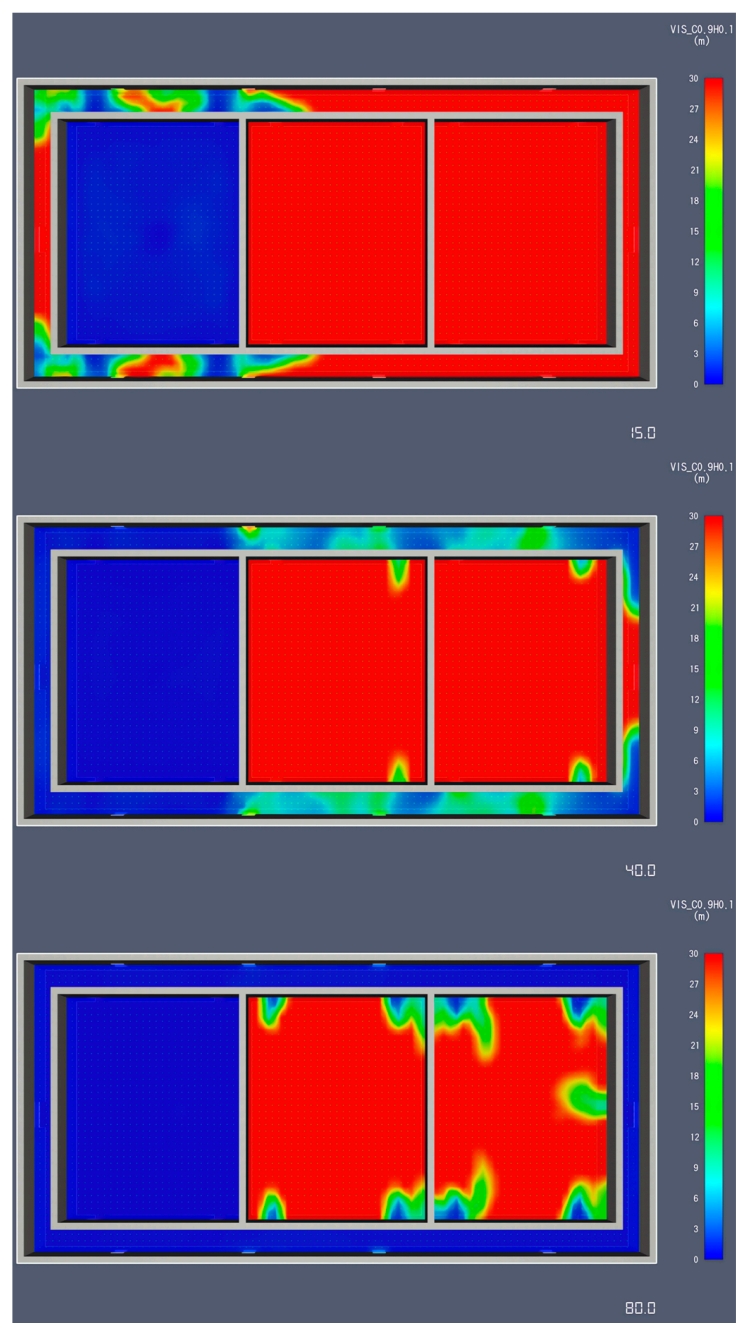


Figure 12. Visibility Schematic of floor scenario.

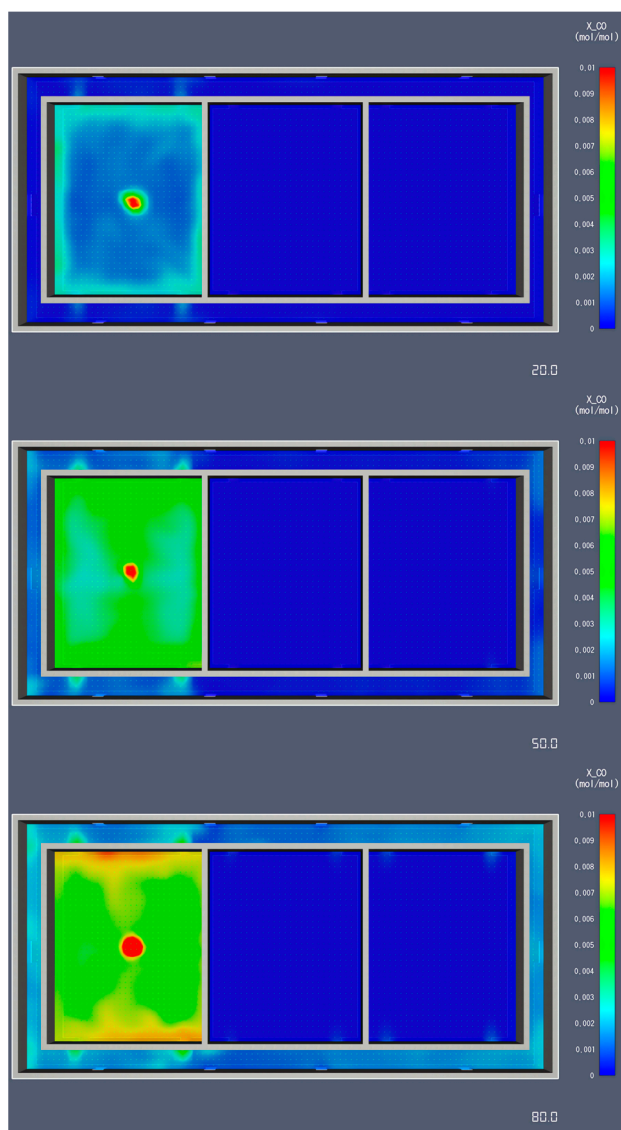


Figure 13. CO concentration of floor scenario.

3.2. Effect of Smoke on Evacuation Times

Figures 14 and 15 show the evacuation of pedestrians when the smoke effect is different. Analyzing the data in Figure 14, it can be seen that the pedestrians in the room completed their evacuation in 43 s when there was no smoke interference. At the beginning of the fire, the smoke concentration in the scene was low and did not significantly affect the movement speeds of the pedestrians, so there was no significant difference in the evacuation of pedestrians under each condition, and the number of people who completed evacuation per unit of time was the same. At 23 s, the visibility range began to affect the movement speeds of pedestrians, and the number of pedestrians evacuated per unit of time decreased significantly. After 30 s, the effect of CO on the movement speeds of pedestrians gradually appeared and began to adversely affect the evacuation of the pedestrians. Considering the effects of smoke visibility and CO on pedestrian evacuation at the same time, it can be found that the effect of smoke visibility on pedestrian evacuation plays a dominant role. The prolonged effect of CO on pedestrian evacuation is about 16%, the prolonged effect of visibility on pedestrian evacuation is about 50%, and the prolonged effect of smoke interference on pedestrian evacuation is about 68%. As can be seen in Figure 15, the effect of smoke on pedestrians is longer in the multi-room scenario than in the single-room scenario, and the effect of CO is more pronounced, resulting in longer pedestrian evacuation times

with smoke interference than when only visibility is considered. The prolonged effect of CO on pedestrian evacuation is about 40%, the prolonged effect of visibility on pedestrian evacuation is about 106%, and the prolonged effect of smoke interference on pedestrian evacuation is about 168%.

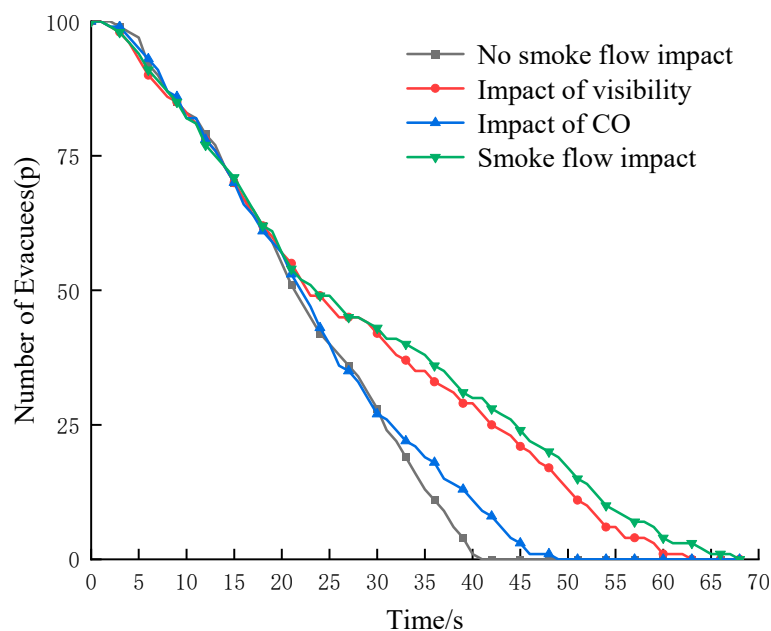


Figure 14. Evacuation situation of room scenario.

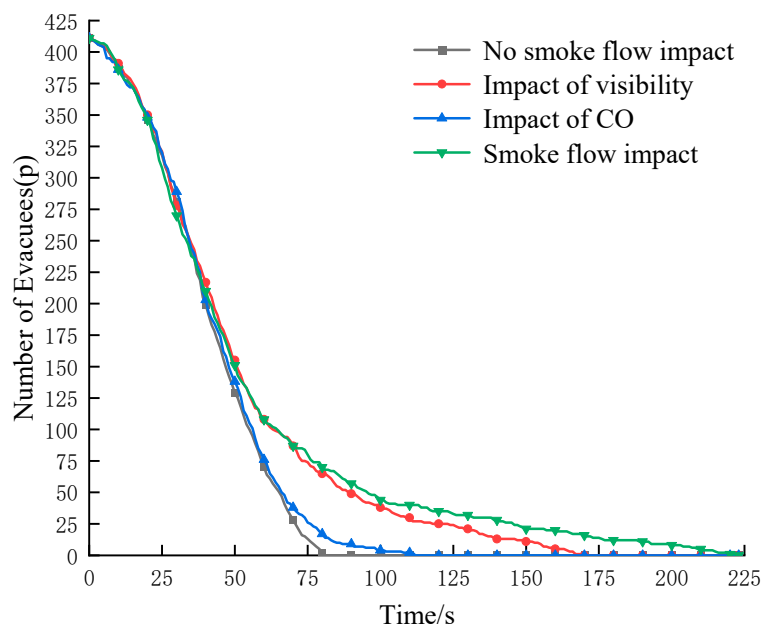


Figure 15. Evacuation situation of floor scenario.

3.3. Coupled Effects of Pedestrian Visibility and Site Familiarity on Pedestrian Evacuation

In the event of a fire, the evacuation time for pedestrians varies based on their familiarity with the location. Different levels of familiarity affect the way pedestrians move during the evacuation [31]. Pedestrians who are familiar with the scenario tend to take the shortest route to the exit, while those who are unfamiliar with the scenario rely on cues within their field of view to determine their movement. Pedestrians with a herd mentality

are influenced by the distribution of other pedestrians in their field of view and move accordingly, while those with a rational mentality follow the direction indicated by fire signs in their field of view. In the absence of cues, pedestrians tend to move toward the walls and proceed in a particular direction along the wall.

To investigate the pedestrian evacuation process under the dynamic changes in the visibility range coupled with pedestrian familiarity, cellular automata models are established for different pedestrian densities (ρ) in various scenarios. Figure 16 illustrates the variation in the pedestrian evacuation time step concerning the proportion (λ) of initially familiar pedestrians in the single-room scenario at different pedestrian densities. The analysis of simulation data reveals that higher crowd familiarity leads to a faster complete evacuation time. At pedestrian densities of 0.4 and 0.5, with a crowd familiarity of 0.3, the evacuation time slightly decreases due to familiar pedestrians quickly reaching and leaving the exit. Conversely, unfamiliar pedestrians face limited visibility, resulting in reduced pedestrian density near the exit and alleviating congestion caused by the arching effect. The effect of the combined effects of crowd visibility and venue familiarity in the multi-room scenario is shown in Figure 17. Analyzing the data in Figure 17, it can be seen that the time required for complete pedestrian evacuation in the multi-room scenario continues to decrease as λ increases.

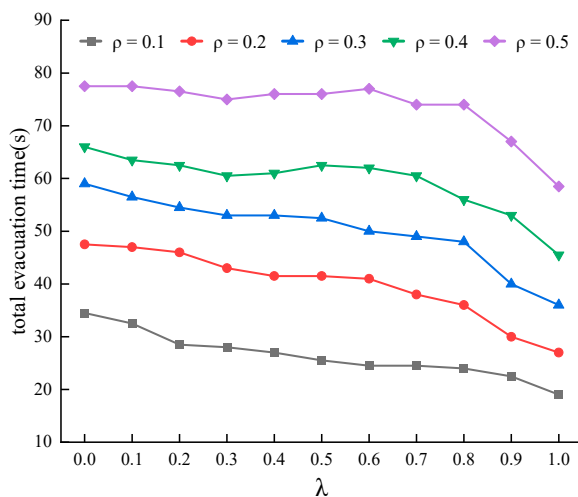


Figure 16. Pedestrian evacuation time in the room scenario.

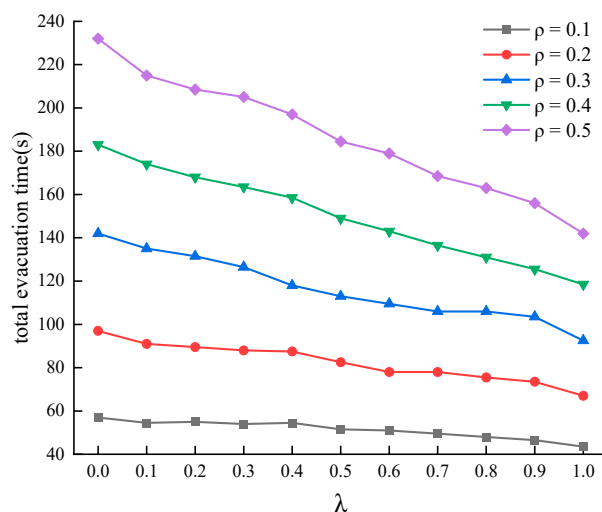


Figure 17. Pedestrian evacuation time in the floor scenario.

Crowd familiarity under different pedestrian densities does not have the same effect on evacuation. The improvement in pedestrian evacuation efficiency under different scenarios is shown in Table 2. In the single-room scenario, as the pedestrian density increases from 0.1 to 0.5, the impact of crowd familiarity on improving evacuation efficiency gradually diminishes, declining from 44.93% to 24.52%. The effect of crowd familiarity on evacuation efficiency continues to decrease as pedestrian density increases. Conversely, in the multi-room scenario, as pedestrian density increases from 0.1 p/m² to 0.5 p/m², the improvement effect of crowd familiarity on evacuation efficiency increases from 23.68% to 38.79%. However, similar to the single-room scenario, the improvement effect of crowd familiarity on evacuation efficiency starts to decrease as pedestrian density increases. The dynamics of complex terrain contribute to this phenomenon. As the number of pedestrians in the venue increases, the likelihood of information exchange between familiar and unfamiliar pedestrians also increases. This facilitates the guidance of unfamiliar pedestrians by those familiar with the venue, leading them to follow others in the evacuation process, thereby increasing the overall efficiency of pedestrian evacuation.

Table 2. Evacuation efficiency.

Pedestrian Density	The Room Scenario			The Floor Scenario		
	Complete Pedestrian Evacuation Time at $\lambda=0$	Complete Pedestrian Evacuation Time at $\lambda=1$	Enhanced Efficiency	Complete Pedestrian Evacuation Time at $\lambda=0$	Complete Pedestrian Evacuation Time at $\lambda=1$	Enhanced Efficiency
0.1	34.5	19	44.93%	57	43.5	23.68%
0.2	47.5	27	43.16%	97	67	30.93%
0.3	59	36	38.98%	142	92.5	34.86%
0.4	66	45.5	31.06%	183	118.5	35.25%
0.5	77.5	58.5	24.52%	232	142	38.79%

3.4. Pedestrian Victimization Analysis

In reality, renovated structures consist of a variety of materials, so the CO produced after a fire does not occur at fixed rates. This section investigates pedestrian casualties when CO production rates vary. To investigate this aspect, the FDS-based Pyrosim software is utilized to simulate the distribution of CO in the scene, considering CO production rates ranging from 0.02 to 0.20. Two pedestrian evacuation models are created to analyze the effects of crowd familiarity (ω) on pedestrian casualties. The parameter ω represents the proportion of pedestrians in the crowd who are familiar with the scene. One model sets $\omega = 1$, representing high crowd familiarity, while the other model sets $\omega = 0.3$, representing low crowd familiarity. This study calculates the increase in HbCO concentration in the bodies of pedestrians based on the CO concentration at their respective locations during the evacuation process. In addition, the dwell time and exposure of pedestrians to CO during the evacuation are thoroughly analyzed.

Figure 18 shows the high familiarity crowd casualties in the indoor scenario. The data show that the number of pedestrians with zero HbCO concentration in their bodies ranges from seven to nine at different CO production rates. Pedestrians with an HbCO concentration greater than 0.1 began to appear at a CO yield of 0.14, and their numbers increased at higher CO yields. As the CO yield increased, the population numbers in each HbCO concentration range first increased and then decreased. Figure 19 shows the victimization of the low-familiarity crowd in the room fire scenario. The number of pedestrians with no HbCO concentration in the body was not substantially impacted by increasing the CO yield. When the CO production rate was less than 10%, the number of pedestrians with an HbCO concentration of less than 0.001 showed a noticeable decreasing trend with higher CO production rates. At the same time, the number of pedestrians with an HbCO concentration between 0.001 and 0.01 in their bodies showed a significant increase, followed by a stabilization of the trend.

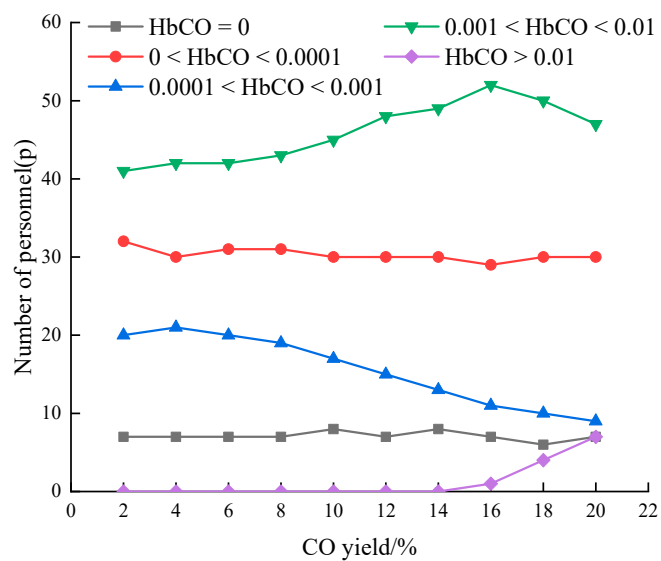


Figure 18. Victimization of high familiarity in room scenario.

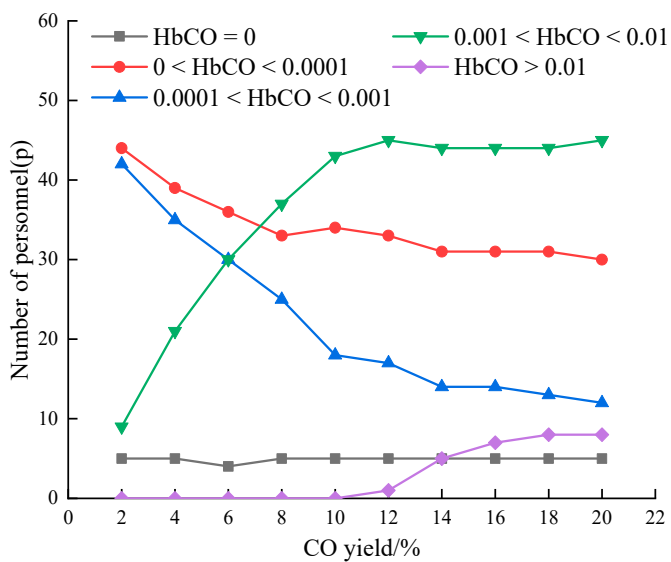


Figure 19. Victimization of low familiarity in room scenario.

Comparing Figures 18 and 19, the number of pedestrians with a body HbCO concentration of zero is lower in the low-familiarity population than in the high-familiarity population. This means that the fewer people who know about the fire, the fewer people who will be exposed to CO. When the CO yield in smoke is less than 10%, the low-familiarity population has a higher number of pedestrians with body HbCO concentrations less than 0.001 and in the range of 0.001 to 0.01 compared to the high-familiarity population. Pedestrians familiar with the site tend to choose the shortest path through the smoke to evacuate the premises. Consequently, when the CO production rate is low and the smoke concentration at the scene is minimal, pedestrians who traverse through the smoke have higher body HbCO concentrations than those who evacuate away from the smoke along the walls. However, it takes longer for the crowd with low exposure to evacuate. As the CO production rate increases, smoke diffusion leads to higher CO concentrations in the room, resulting in pedestrians with body HbCO concentrations greater than 0.01 appearing earlier than the high-familiarity crowd.

Pedestrian casualties in the high-familiarity and low-familiarity populations at different CO yield rates in the multi-room scenario are shown in Figures 20 and 21, respectively.

A comprehensive analysis of Figures 20 and 21 shows that the number of pedestrians with HbCO concentrations less than 0.01 in the low-familiarity population is higher than that in the high-familiarity population at different CO production rates. And the number of pedestrians with an HbCO concentration greater than 0.1 in the low-familiarity population is greater than that in the high-familiarity population. Moreover, as the CO production rate increases, the number of pedestrians with lower HbCO concentrations decreases and stabilizes, while the number of pedestrians with higher HbCO concentrations increases.

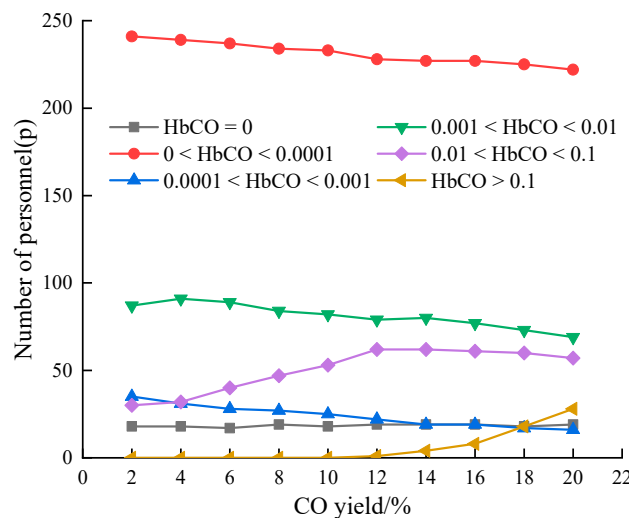


Figure 20. Victimization of high familiarity in floor scenario.

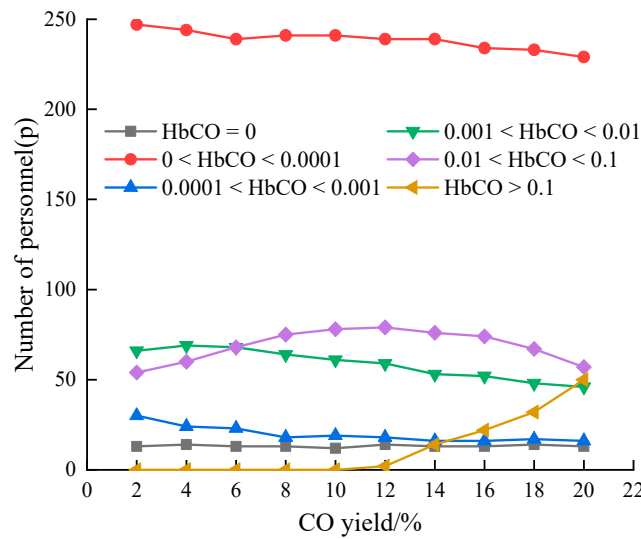


Figure 21. Victimization of low familiarity in floor scenario.

4. Conclusions

- (1) The traditional pedestrian evacuation model faces the challenge of accurately representing speed variations in different environments. To address this issue, we propose a novel approach by integrating fire dynamics software, resulting in a dynamic cellular automaton evacuation model with adaptive pedestrian movement parameters. This model allows for real-time updates of pedestrian movement parameters, leading to a more realistic simulation of pedestrian evacuation scenarios in real fire situations.
- (2) The evacuation efficiency of pedestrians during a fire is influenced by crowd familiarity, and higher crowd familiarity correlates with shorter evacuation time. In the single-room scenario, as the population density increases from 0.1 to 0.5, the effect

of crowd familiarity on evacuation efficiency decreases from 44.93% to 24.52%. Conversely, in the multi-room scenario, the effect of crowd familiarity on evacuation efficiency increases from 23.68% to 38.79%.

- (3) During the initial stages of a fire, smoke has little effect on pedestrian movement speed and does not significantly affect pedestrian evacuation efficiency. However, smoke visibility plays a critical role in determining pedestrian movement speed and can increase evacuation time by more than 50%. In addition, CO significantly affects pedestrian evacuation in scenarios with longer evacuation times. We found that pedestrian familiarity can reduce the number of people affected by CO. Additionally, as the CO production rate increases, the percentage of pedestrians less affected by smoke aggression in the crowd decreases and stabilizes.

Author Contributions: Conceptualization, Y.L. and C.S.; methodology, C.S.; software, J.L.; validation, C.S. and Y.L.; formal analysis, J.L.; investigation, C.S.; data curation, J.L.; writing—original draft preparation, J.L.; writing—review and editing, Y.L.; supervision, Y.L.; project administration, C.S. All authors have read and agreed to the published version of the manuscript.

Funding: This research was funded by the National Natural Science Foundation of China (11704090), University Nursing Program for Young Scholars with Creative Talents in Heilongjiang Province (UNPYSC-2018207), and the project of Nature Scientific Foundation of Heilongjiang Province (LH2020A016).

Institutional Review Board Statement: Not applicable.

Informed Consent Statement: Not applicable.

Data Availability Statement: The data used in this study are available on request from the corresponding author.

Conflicts of Interest: The authors declare no conflict of interest.

References

1. Von Schantz, A.; Ehtamo, H. Minimizing the evacuation time of a crowd from a complex building using rescue guides. *Phys. A Stat. Mech. Its Appl.* **2022**, *594*, 127011. [[CrossRef](#)]
2. Kuti, R.; Zólyomi, G.; László, G.; Hajdu, C.; Környei, L.; Hajdu, F. Examination of effects of indoor fires on building structures and people. *Heliyon* **2023**, *9*, e12720. [[CrossRef](#)] [[PubMed](#)]
3. Medved, S.; Medved, S. Buildings Fires and Fire Safety. In *Building Physics: Heat, Ventilation, Moisture, Light, Sound, Fire, and Urban Microclimate*; Springer Nature: Berlin, Germany, 2022; pp. 407–451.
4. Long, X.; Zhang, X.; Lou, B. Numerical simulation of dormitory building fire and personnel escape based on Pyrosim and Pathfinder. *J. Chin. Inst. Eng.* **2017**, *40*, 257–266. [[CrossRef](#)]
5. Xiao, M.; Zhou, X.; Pan, X.; Wang, Y.; Wang, Y.; Li, X.; Sun, Y.; Wang, Y. Simulation of emergency evacuation from construction site of prefabricated buildings. *Sci. Rep.* **2022**, *12*, 2732. [[CrossRef](#)]
6. Liu, Z.; Gu, X.; Hong, R. Fire protection and evacuation analysis in underground interchange tunnels by integrating BIM and numerical simulation. *Fire* **2023**, *6*, 139. [[CrossRef](#)]
7. Jiang, S.; Wang, C.; Bimenyimana, S.; Boon, J.; Zhang, G.; Li, H. Standard operational procedures (SOP) for effective fire safety evacuation visualization in college dormitory buildings. *J. Vis.* **2021**, *24*, 1207–1235. [[CrossRef](#)]
8. Shams Abadi, S.T.; Moniri Tokmehdash, N.; Hosny, A.; Nik-Bakht, M. BIM-based co-simulation of fire and occupants' behavior for safe construction rehabilitation planning. *Fire* **2021**, *4*, 67. [[CrossRef](#)]
9. Jasztal, M.; Omen, Ł.; Kowalski, M.; Jaskółkowski, W. Numerical simulation of the airport evacuation process under fire conditions. *Advances in Science and Technology. Res. J.* **2022**, *16*, 249–261.
10. Zisis, T.; Vasilopoulos, K.; Sarris, I. Effect of Passenger Physical Characteristics in the Uptake of Combustion Products during a Railway Tunnel Evacuation Due to a Fire Accident. *Computation* **2023**, *11*, 82. [[CrossRef](#)]
11. Liao, L.; Li, H.; Li, P.; Bao, X.; Hong, C.; Wang, D.; Xie, X.; Fan, J.; Wu, P. Underground Evacuation and Smoke Flow Simulation in Guangzhou International Financial City during Fire. *Fire* **2023**, *6*, 266. [[CrossRef](#)]
12. Zhou, M.; Zhou, B.; Zhang, Z.; Zhou, Z.; Liu, J.; Li, B.; Wang, D.; Wu, T. Fire Egress System Optimization of High-Rise Teaching Building Based on Simulation and Machine Learning. *Fire* **2023**, *6*, 190. [[CrossRef](#)]
13. Zhang, N.; Liang, Y.; Zhou, C.; Niu, M.; Wan, F. Study on Fire Smoke Distribution and Safety Evacuation of Subway Station Based on BIM. *Appl. Sci.* **2022**, *12*, 12808. [[CrossRef](#)]
14. Neumann, J.; Burks, W. *Theory of Self-Reproducing Automata*; Urbana; University of Illinois Press: Champaign, IL, USA, 1966.

15. Wen, G.; Hong, Y.; Wei, C. A cellular automaton evacuation model based on mobile robot's behaviors. *Chin. Sci. Bull.* **2007**, *52*, 680–684.
16. Wang, C.; Tang, Y.; Kassem, M.A.; Li, H.; Wu, Z. Fire evacuation visualization in nursing homes based on agent and cellular automata. *J. Saf. Sci. Resil.* **2021**, *2*, 181–198. [[CrossRef](#)]
17. Fu, Z.; Yang, L.; Chen, Y.; Zhu, K.; Zhu, S. The effect of individual tendency on crowd evacuation efficiency under inhomogeneous exit attraction using a static field modified FFCA model. *Phys. A Stat. Mech. Its Appl.* **2013**, *392*, 6090–6099. [[CrossRef](#)]
18. Kontou, P.; Georgoulas, I.G.; Trunfio, G.A.; Sirakoulis, G.C. Cellular automata modelling of the movement of people with disabilities during building evacuation. In Proceedings of the 26th Euromicro International Conference on Parallel, Distributed, and Network-Based Processing, PDP, Cambridge, UK, 21–23 March 2018; pp. 550–557.
19. Miyagawa, D.; Ichinose, G. Cellular automaton model with turning behavior in crowd evacuation. *Phys. A Stat. Mech. Its Appl.* **2020**, *549*, 124376. [[CrossRef](#)]
20. Martha, M.; Nikolaos, I.D.; Georgios, C.S.; Katsuhiro, N. Spatial games and memory effects on crowd evacuation behavior with Cellular Automata. *J. Comput. Sci.* **2019**, *32*, 87–98.
21. Khandoker, M.A.R.; Mou, R.J.; Muntaha, M.A.; Rahman, M.A. Numerical simulation of fire in a multistoried ready-made garments factory using PyroSim. In Proceedings of the International Conference on Mechanical Engineering: Proceedings of the 12th International Conference on Mechanical Engineering (ICME 2017), Dhaka, Bangladesh, 20–22 December 2017; AIP Conference Proceedings; AIP Publishing: Melville, NY, USA, 2018; Volume 1980.
22. Xu, M.; Peng, D. Pyrosim-based numerical simulation of fire safety and evacuation behaviour of college buildings. *Int. J. Saf. Secur. Tour.* **2020**, *10*, 293–299. [[CrossRef](#)]
23. Jeon, G.Y.; Kim, J.Y.; Hong, W.H.; Augenbroe, G. Evacuation performance of individuals in different visibility conditions. *Build. Environ.* **2011**, *46*, 1094–1103. [[CrossRef](#)]
24. Liu, Y.; Mao, Z. An experimental study on the critical state of herd behavior in decision-making of the crowd evacuation. *Phys. A Stat. Mech. Its Appl.* **2022**, *595*, 127087. [[CrossRef](#)]
25. Alex, R.; Alessandro, L. Clustering by fast search and find of density peaks. *Science* **2014**, *344*, 1492–1496.
26. Tanizaki, S. Assessing inhalation injury in the emergency room. *Open Access Emerg. Med.* **2015**, *7*, 31–37. [[CrossRef](#)] [[PubMed](#)]
27. Usta, N. Investigation of fire behavior of rigid polyurethane foams containing fly ash and intumescence flame retardant by using a cone calorimeter. *J. Appl. Polym. Sci.* **2012**, *124*, 3372–3382. [[CrossRef](#)]
28. Qiu, R.; Fan, W. Biological toxicology of harmful reactive products in fire(I): Carbon monoxide, hydrocyanic acid. *Fire Saf. Sci.* **2001**, *10*, 154–158.
29. Anastasios, K.; Despina, P.; Nikolas, G.; Kaliampakos, D. Evacuation in an underground Space: A real-time investigation of occupants' travel speed in clear and smoked environments. *Infrastructures* **2022**, *7*, 57. [[CrossRef](#)]
30. Ye, C.; Liu, Y.; Sun, C. Risk Assessment of Pedestrian Evacuation under the Influence of Fire Products. *Discret. Dyn. Nat. Soc.* **2020**, *2020*, 9540942. [[CrossRef](#)]
31. Tong, Y.; Bode, N.W.F. The principles of pedestrian route choice. *J. R. Soc. Interface* **2022**, *19*, 20220061. [[CrossRef](#)]

Disclaimer/Publisher's Note: The statements, opinions and data contained in all publications are solely those of the individual author(s) and contributor(s) and not of MDPI and/or the editor(s). MDPI and/or the editor(s) disclaim responsibility for any injury to people or property resulting from any ideas, methods, instructions or products referred to in the content.